ELSEVIER

Colloids and Surfaces
A: Physicochemical and Engineering Aspects 149 (1999) 245–251

COLLOIDS AND SURFACES A

Motion of a massive particle attached to a spherical interface: statistical properties of the particle path

K. Velikov [a], K. Danov [a], M. Angelova [b], C. Dietrich [c], B. Pouligny [c,*]

[a] *Laboratory of Thermodynamics and Physico-Chemical Hydrodynamics, University of Sofia, 1126 Sofia, Bulgaria*
[b] *Institute of Biophysics, Bulgarian Academy of Sciences, Acad. G. Bonchev str., 1113 Sofia, Bulgaria*
[c] *Centre de Recherche Paul-Pascal, av. A. Schweitzer, 33600 Pessac, France*

Received 3 September 1997; accepted 25 June 1998

Abstract

We have studied the motion of a Brownian particle on a spherical interface under gravity, with the aim of setting up a protocol to measure the friction (ζ) felt by such a particle in experimental conditions. Our analysis is based on the Schmoluchowski equation for particle motion. Essentially we derive a practical criterion to find ζ from the average particle path. Our statements are illustrated by a few experimental and numerical examples. Numerical paths are obtained by computer simulation and experimental paths are those of micrometre-sized latex or glass particles attached to spherical giant lipid (SOPC) vesicles. From experimental values of ζ, we estimate the surface shear viscosity of SOPC bilayers to be in the range $3–8 \times 10^{-6}$ Poise.

Keywords: Brownian motion; Lipid vesicles; Membrane viscosity

1. Introduction

Recently, it was shown by Angelova et al. [1] and Dietrich et al. [2] that micrometre-sized spheres of polystyrene or glass could be attached to lipid bilayers without any special surface treatment. In these experiments, a particle was manipulated by means of an optical trap [3] and brought in contact with a spherical giant vesicle [4] about 50 μm in size. Usually the particle stabilizes itself across the vesicle contour, with a finite contact angle (α). Adhesion dynamics may feature different steps [2], but after equilibrium has been achieved, α takes on a constant value. This value is not universal, as it depends strongly on the initial vesicle tension and the nature of the particle surface. A typical situation is shown in Fig. 1; here α is far from 0 or 180°, which means that the particle intercepts a definite portion of the vesicle contour.

If the membrane is in the fluid state (this is so, for instance, with egg lecithin at room temperature), the particle can still be moved along the vesicle contour by means of the optical trap. In our experiments, we bring the particle near the top of the vesicle and release it by switching off the optical trap. Then it starts moving down, as shown in Fig. 2. In such an experiment, the particle plays the role of a macroscopic mechanical probe, which may be used to feel the friction opposed by the membrane to its motion.

If this friction is measured, one may then deduce the membrane shear viscosity with the help of an appropriate theory [5]. At this time, the theory

* Corresponding author. Tel.: +33-0556-845683; fax: +33-0556-845600; e-mail: pouligny@crpp.u-bordeaux.fr

0927-7757/99/$ – see front matter
PII S0927-7757(98)00604-9

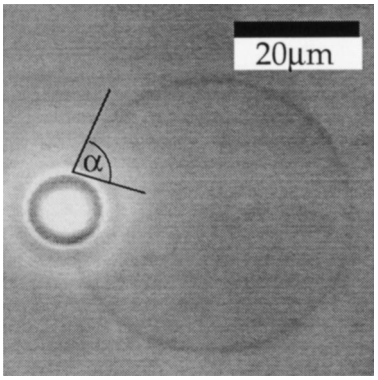

Fig. 1. Example of a latex particle attached to a giant SOPC vesicle. Here the contact angle (α) is about 80°. The particle is homogeneous. The apparent composite structure (black and white circular zones) is an artefact owing to phase contrast microscopy.

closest to our need is that of Danov et al. [6], which depicts the motion of a spherical particle across a Langmuir film at the water/air interface. To apply the theory requires that the interface be flat and infinite, which means that the particle radius (a) must be much smaller than the vesicle radius (R). Conversely, the experimental procedure requires the particle to be large enough for the contact angle to be resolved by optical microscopy. These opposite requirements lead to a trade-off in the particle size, which is of the order of 1 or 2 μm. Such particles are heavy enough to definitely "sediment" down to the bottom of the vesicle but small enough to undergo highly visible Brownian excursions in the same time. An example of such a "hybrid" motion is shown in Fig. 2.

The purpose of this paper is to outline some relevant statistical properties of these hybrid paths and to propose a practical way of extracting the particle friction coefficient. Essentially, we want to justify the procedure that was used in [5] to measure friction coefficients of latex microspheres on SOPC (L_α-stearoyl-oleoyl-phosphatidylcholine) bilayers. In principle, this contribution goes beyond the scope of the particular system used in our experiments — i.e., particles on lipid vesicles — as it mainly addresses the more general problem of a *massive random walker on a spherical surface*.

The following section is purely analytical: we start from the Schmoluchowski equation for the particle position probability density and derive a

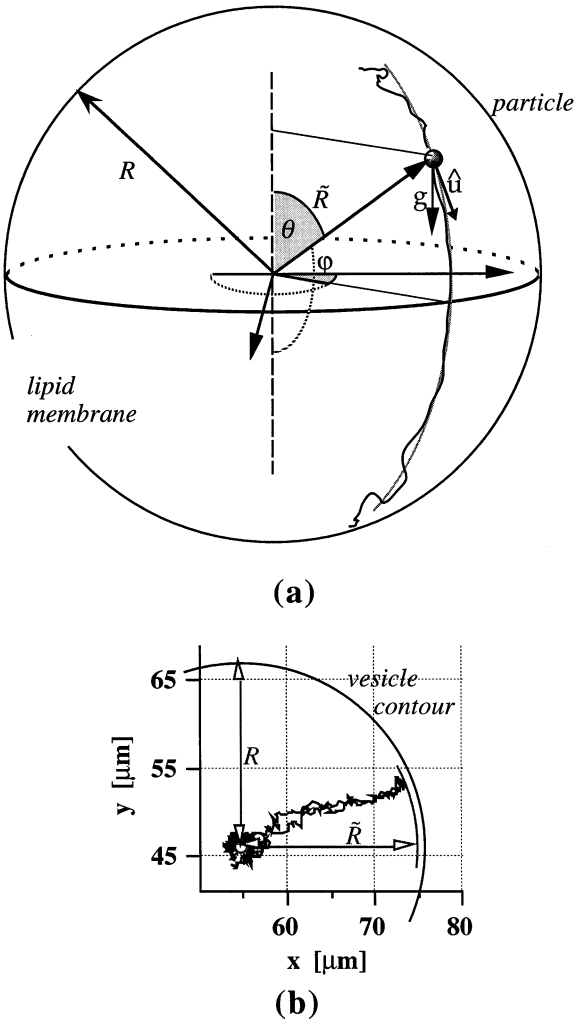

Fig. 2. (a) Schematic representation of the trajectory of a massive Brownian particle on a spherical vesicle. (b) Example of an experimental record with a glass particle (radius $a=1.21$ μm). The vesicle radius is $R=21.2$ μm.

general equation for particle average trajectories and Brownian excursions. Our statements are illustrated in Section 3 by means of a few experimental and numerical examples. Section 4 presents our conclusions.

2. Theory

A priori, the problem of a finite-sized spherical particle moving along a membrane involves both

translation and rotation of the particle relative to the membrane and the surrounding fluid. In fact, experiments carried out by Dietrich et al. [2] on ''three-body'' systems, either a particle with two vesicles or two particles on a single vesicle, indicate that the membrane–particle contact line is pinned to the particle surface. This is observed in the most common situation, when the particle is only partially wetted by the membrane material. Consequently the particle cannot move radially (the contact angle is constant) and cannot rotate relative to the contact line.

This simplifies the model greatly, as only two translational degrees of freedom, namely the polar angles (ϕ,θ) defined in Fig. 2, are necessary to define the particle position. This reduces the problem to that of a massive point random walker on a spherical surface.

We base our analysis on the Schmoluchowski equation for a diffusing particle in an external field (e.g., [7,8]):

$$\frac{\partial w}{\partial t} = \mathrm{div}\left[D\,\mathrm{grad}(w) - \frac{\tilde{m}g\cdot\sin\theta}{\zeta}\,\hat{u}w \right] \tag{1}$$

where $w(\theta,\phi,t)$ is the probability density for the particle to be at position (ϕ,θ) at time t. w is 2π-periodic in θ and ϕ and is normalized according to:

$$\int_0^{\pi} \sin\theta\,\mathrm{d}\theta \int_0^{2\pi} \mathrm{d}\phi\cdot w = 1 \tag{2}$$

The quantity in brackets in Eq. (1) is the sum of a linear diffusive flux and a gravity-driven convective flux. D and ζ are the particle diffusion and friction coefficients, respectively. $\tilde{m}g$ is the particle weight corrected for buoyancy. Note that the Einstein relation reads $D=kT/\zeta$, where k is the Boltzmann constant and T the absolute temperature. In our problem, the particle is constrained to move on a sphere of radius $\tilde{R}$, which is the distance between the particle and vesicle centres in the physical situation (Fig. 2). $\hat{u}$ is the unit vector parallel to the vesicle surface in the $(\tilde{R},g)$ plane (see Fig. 2(a)).

Let us denote $x=\cos\theta$, replace the probability $w(\theta,\phi,t)\sin\theta\,\mathrm{d}\theta\,\mathrm{d}\phi$ by $w(x,\phi,\tau)\,\mathrm{d}x\,\mathrm{d}\phi$ and define a dimensionless time as:

$$\tau = t\cdot\tilde{m}g/\tilde{R}\zeta \tag{3}$$

Writing Eq. (1) in spherical coordinates, we obtain:

$$\frac{\partial w}{\partial \tau} = \frac{\partial}{\partial x}\left[\left(1-x^2\right)w\right] + \frac{1}{Pe}\left\{\frac{\partial}{\partial x}\left[\left(1-x^2\right)\frac{\partial w}{\partial x}\right] + \frac{1}{1-x^2}\frac{\partial^2 w}{\partial \phi^2}\right\} \tag{4}$$

In Eq. (4) Pe is the so-called ''Peclet number'', which we define here as $Pe=\tilde{m}g\cdot\tilde{R}/kT$. Notice that $\tilde{m}g\cdot\tilde{R}$ is the variation of the particle gravitation energy when it moves from, say, the vesicle top down to the equatorial plane. Thus Pe is the ratio of a sedimentation energy to the thermal energy. The first term on the right-hand side of Eq. (4) represents the zero-temperature limit of the equation. The second term arises from Brownian noise. Let $f(x)$ be a function that depends on θ only and

$$\langle f\rangle = \int_0^{2\pi}\mathrm{d}\phi\int_{-1}^{+1}\mathrm{d}x\,f(x)w(x,\phi,\tau) \tag{5}$$

be the ensemble average of f. Combining Eqs. (4) and (5) and three integrations by part lead to the following general property:

$$\frac{\mathrm{d}}{\mathrm{d}\tau}\langle f\rangle = -\left\langle\left(1-x^2\right)\frac{\mathrm{d}f}{\mathrm{d}x}\right\rangle + \frac{1}{Pe}\left\langle\frac{\mathrm{d}}{\mathrm{d}x}\left[\left(1-x^2\right)\frac{\mathrm{d}f}{\mathrm{d}x}\right]\right\rangle - \frac{2\pi}{Pe}\left[h(1,\phi,\tau)-h(-1,\phi,\tau)\right] \tag{6}$$

with $h(x,\phi,\tau)=(1-x^2)\ \mathrm{d}f/\mathrm{d}x\ w(x,\phi,\tau)$. Eq. (6) holds provided that $(1-x^2)f(x)\to 0$ when $x\to\pm 1$. A most relevant example is $f(x)=a\tanh[\cos\theta(t)]$, which gives:

$$\frac{\mathrm{d}}{\mathrm{d}\tau}\langle a\tanh[\cos\theta(t)]\rangle = -1 - \frac{2\pi}{Pe}\left[w(1,\phi,\tau)-w(-1,\phi,\tau)\right] \tag{7}$$

Note that $2\pi w(\pm 1,\phi,\tau)\mathrm{d}x$ is the probability for the particle centre to be within a distance $\tilde{R}\,\mathrm{d}x$ of the vesicle top or bottom; i.e., such that $1-\mathrm{d}x \le x \le 1$ or $-1 \le x \le -1+\mathrm{d}x$, respectively. In the $Pe\to\infty$ (or $T\to 0$) limit, there is no Brownian noise and the trajectory becomes deterministic. In this limit, Eq. (7) becomes:

$$\frac{\mathrm{d}}{\mathrm{d}\tau}\, a\tanh[\cos\theta(\tau)] = -1 \tag{8}$$

This result can be arrived at directly from the mechanical equation of particle motion:

$$\tilde{m}g\sin\theta = \zeta\tilde{R}\frac{\mathrm{d}\theta}{\mathrm{d}t} \tag{9}$$

Eq. (9) expresses the balance between the particle effective weight, i.e., the component parallel to $\hat{u}$, and the friction force, $\zeta\tilde{R}\,\mathrm{d}\theta/\mathrm{d}t$. In Eq. (9) we neglected the acceleration force (i.e., inertia) because the particle velocities involved in the experiments are very small (the Reynolds number is of the order of 10^{-4} or less). Integration of Eq. (8) (or equivalently Eq. (9) gives:

$$a\tanh[\cos\theta(t)] = a\tanh[\cos\theta_0] - \frac{\tilde{m}g}{\tilde{R}\zeta}\,t \tag{10}$$

Here θ_0 is the particle azimuthal angle at time origin. Eq. (10) represents the "zero-temperature" limit of the motion.

In the general situation, the second term on the right-hand side of Eq. (7) is responsible for a systematic deviation between the average path and the $T\to 0$ limit path when Pe is finite. This deviation occurs whenever the probability density that the particle will be at the vesicle top ($x=1$) or bottom ($x=-1$) is not negligible compared with Pe. Of course this situation is favoured for small particles, because Pe is small and Brownian excursions are large enough for the particle to reach a pole of the vesicle.

In the experiments and simulations (see Section 3), the particle is released at time $\tau=\tau_0$ from a position definitely above the vesicle equatorial plane ($\theta_0<\pi/2$). At $\tau=\tau_0$, i.e., just when the particle is released, w is nil everywhere except at $\theta=\theta_0$, $\phi=\phi_0$. Then $w(\pm 1,\phi,\tau_0)=0$ and the slope in $\langle a\tanh[\cos\theta(t)]\rangle$ is predicted to be -1. However, at $\tau>\tau_0$, Brownian excursions start immediately and $w(1,\phi,\tau)$ starts increasing. If θ_0 is very small (as in the simulations, see Section 3), the influence of gravity shortly after τ_0 is very weak and the particle motion can be viewed roughly as a pure diffusion on a flat surface. In this limit,

$$w(1,\phi,t) \cong \frac{\tilde{R}^2}{4\pi Dt}\exp\left[-\frac{(\tilde{R}\theta_0)^2}{4Dt}\right] \tag{11}$$

From Eq. (11), we expect $(2\pi/Pe)w(1,\phi,\tau)$ to reach a maximum

$$(2\pi/Pe)w_{\mathrm{m}} \cong \frac{0.74}{Pe\cdot\theta_0^2} \tag{12a}$$

within a time

$$\tau_{\mathrm{m}} - \tau_0 \cong Pe\cdot\theta_0^2/4 \tag{12b}$$

after particle release.

The slope of $\langle a\tanh(\cos\theta)\rangle$ remains steeper than -1 as long as $w(1,\phi,\tau)>w(-1,\phi,\tau)$. Conversely $w(1,\phi,\tau)\ll w(-1,\phi,\tau)$ at large times, and the slope is decreased. When $\tau\to\infty$, the density w tends to the thermodynamic distribution

$$w_\infty(x,\phi) = \frac{Pe}{4\pi\sinh(Pe)}\exp(-Pe\cdot x) \tag{13}$$

and $\langle a\tanh(\cos\theta)\rangle$ tends to its equilibrium limit, which is finite and negative.

To summarize this section, we found a simple expression for the particle path $f(x)=a\tanh(\cos\theta)$ which is linear in time in the zero-temperature limit. Eq. (7) tells us how far the average path $\langle f(x)\rangle$ is from the $T\to 0$ limit, $f_{T\to 0}(x)$. The average path is predicted to be close to $f_{T\to 0}(x)$ whenever the probability that the particle visits the vesicle poles, top or bottom, is small. This probability is obviously smallest when the particle average position is near the vesicle equatorial plane, i.e., when $\langle a\tanh(\cos\theta)\rangle \approx 0$. When Pe is large enough, the average path is expected to be linear in time in a large domain around $\theta=\pi/2$. The value of the particle friction coefficient, ζ, can be found directly from the slope of this linear portion.

When Pe is small, the friction coefficient is found

more conveniently from Brownian excursions (i.e., from the noise of the particle position) than from the average path. Injecting $f(x)=x$ and $f(x)=x^2$ into Eq. (6) yields:

$$\frac{1}{2}\frac{\mathrm{d}}{\mathrm{d}\tau}\left(\langle x\rangle^2\right\rangle-\langle x\rangle^2\Big)=-\langle x\rangle\langle x^2\rangle+\langle x^3\rangle+\frac{1}{Pe}\left(1-\langle x^2\rangle\right) \quad (14)$$

Near any starting point $x_0=\cos\theta_0$, Eq. (14) gives:

$$\frac{\mathrm{d}}{\mathrm{d}t}\left(\langle x^2\rangle-\langle x\rangle^2\right)_0=\frac{2D}{\tilde{R}^2}\sin^2\theta_0 \quad (15)$$

The noise in ϕ can be found directly from Eq. (6). In a similar way, we obtain:

$$\frac{\mathrm{d}}{\mathrm{d}t}\langle\phi^2\rangle_0=\frac{2D}{\tilde{R}^2}\frac{1}{\sin^2\theta_0} \quad (16)$$

Note that Eqs. (15) and (16) hold independently of the gravity field. This means that the noise of the particle position close to any point on the sphere surface (i.e., in the limit $x\to x_0$) is the same as that in the zero-gravity limit.

3. Experimental/numerical paths

A few examples of particle paths (in terms of $a\tanh(\cos\theta)$ versus time), either from real experiments or from computer simulations, are displayed in Figs. 3 and 4.

In the experiments (Fig. 3), the particle path is viewed and video-recorded from above. Basically, the recorded trace is the projection of the particle trajectory in a horizontal plane (x,y) near the vesicle equatorial plane. A particle-tracking software yields the position of the particle centre every 0.2 s with a resolution of ± 0.5 μm. In the example shown in Figs. 2(b) and 3, the particle was made of glass and the Peclet number was $Pe=520$. The vesicles used in the experiments are located at the boundary of a cluster of many other vesicles [2,5]. The solid particle is dropped on the side of the vesicle opposite to the cluster [5], about at mid-distance between vesicle top and contour (this corresponds to $\theta_0\approx 30^\circ$). We do so to avoid interactions (including adhesion) of the particle with other vesicles.

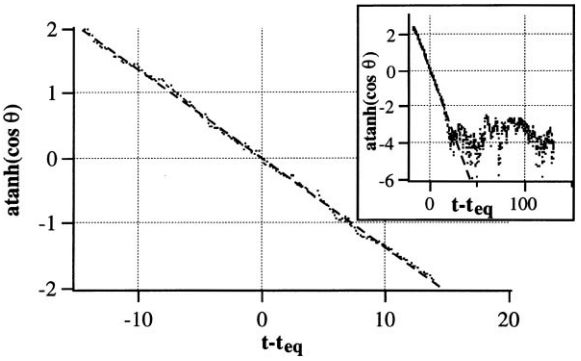

Fig. 3. The path of Fig. 2(b) in $a\tanh[\cos\theta(t)]$ versus time representation. The inset shows the behaviour of the graph at long times.

In the simulations, the time is in dimensionless form (see Eq. (3). The particle trajectories are built in successive time steps: for each step $\delta\tau$ the particle displacement is the sum of a randomly oriented step ($2\sqrt{D\delta\tau}$ in curvilinear distance) and of an elementary sedimentation step, $\delta\theta=(\sin\theta)\delta\tau$. To illustrate the influence of the proximity to the vesicle top pole, the particles were released at $\theta_0\approx 2^\circ$.

In Figs. 3 and 4 the dashed straight lines represent the zero-temperature path, corresponding to Eq. (10). To show the influence of the Peclet number, simulations were performed for different values of Pe from 520 to 6. To illustrate the universality of the average path near the vesicle equatorial plane, the time variable is taken equal to $t-t_{eq}$ in Fig. 3 and to $\tau-\tau_{eq}$ in Fig. 4. Here t_{eq} (in s) or τ_{eq} (dimensionless) is such that $\langle a\tanh[\cos\theta(\tau_{eq})]\rangle=0$. In this representation, all the average trajectories are linear in time and, with the time put in dimensionless form, coincide near τ_{eq}, i.e., near $\theta=\pi/2$, with a slope of -1. As Figs. 3 and 4 show, this is so only in a limited time interval or, equivalently, in a limited range of θ angles around $\theta=\pi/2$, whose size decreases when Pe decreases. This behaviour is well in line with the analytical prediction (Eq. (7)). Experimentally, the easiest way to extract the value of ζ is from the linear portion of the mean particle path in $a\tanh[\cos\theta(t)]$ versus t representation. To find the

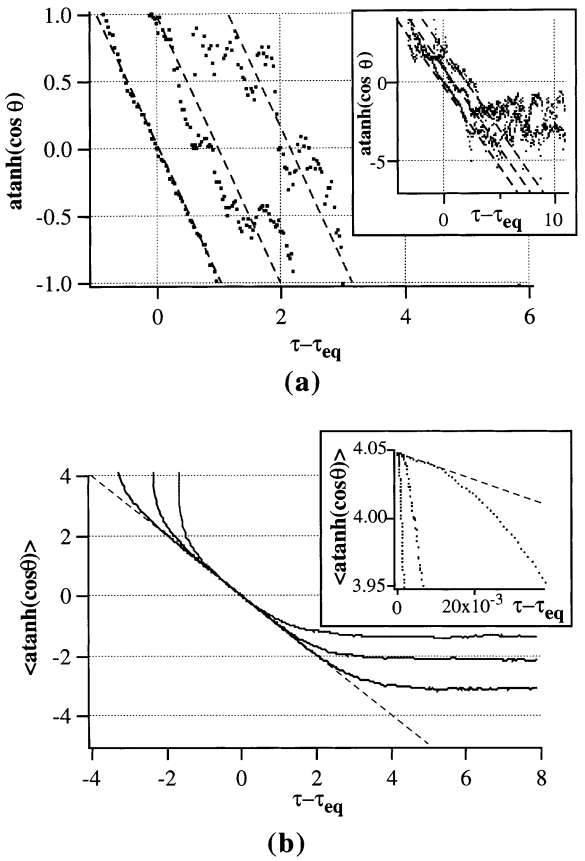

Fig. 4. Examples of particle paths, again in $a\tanh[\cos\theta(t)]$ versus time representation, obtained by numerical simulation, corresponding to $D=0.2\ \mu m^2/s$ and $Pe=180$, 24 and 6, from left to right. The time is in dimensionless form (see text). The dashed straight lines represent the zero-temperature paths (Eq. (10)). (a) Single paths. For clarity, the graphs corresponding to $Pe=24$ and 6 are shifted to the right. The inset shows the behaviour of the graphs at long times. (b) Ensemble averages of $N=1000$ paths for each Pe. Inset: magnified view near τ_0, the instant when the particle is released. Here $N=2\times10^5$, 10^5 and 10^4 for $Pe=6$, 24 and 180, respectively.

value of ζ within a few percent, one needs that the linear portion span at least ±1 rad in θ above and below the vesicle equatorial plane. This requires Pe to be of the order of 100 or more. With polystyrene particles (density ≈1.05), as in ref. [5], this in turn requires a radius $a\geq2\ \mu m$.

At large times, the mean or ensemble average paths deviate from the zero-T path and "plateau" to a finite negative value. One may check that this value coincides with the thermodynamic limit, $\langle a\tanh(\cos\theta)\rangle$, corresponding to the equilibrium distribution (w_∞, Eq. (13)). There is a systematic deviation at small angles too: in this region, the slope of $\langle a\tanh[\cos\theta(t)]\rangle$ is definitely steeper than -1. Note that the maximum steepness is reached only after a finite time (of the order of a few 10^{-3} in dimensionless time) following particle release ($\tau=\tau_0$). This is very clear from the inset in Fig. 4(b), which is a close view of the early parts of particle average trajectories. One may check that the minimum slopes coincide with those estimated from Eqs. (7), (12a) and (12b). For instance, the predicted value is -102 for $Pe=6$, while simulation gives -101.

To summarize, simulations or experiments show that $d\langle a\tanh[\cos\theta(t)]\rangle/d\tau$ initially is close to -1, then decreases rapidly to more negative values, comes back to -1, and finally relaxes to zero in the long time limit. These trends are well in line with the analysis performed in Eq. (2).

4. Conclusion

We have investigated the problem of a random walker on a spherical interface under the influence of gravity. This study is motivated by experiments performed with latex or glass particles attached to giant lipid vesicles. The goal of such experiments is to measure the particle friction coefficient (ζ) on the vesicle surface and ultimately to find the value of the membrane shear viscosity. We drew the conclusion that the pure sedimentation path (defined as the path that the particle would follow in the absence of thermal noise ($T\to0$ limit)) and the mean, or average, path (defined as the ensemble average path) do not coincide, except approximately in a limited domain around the vesicle equatorial plane. If the particle is heavy enough ($Pe>100$), this domain is large and measuring ζ is straightforward. With small particles ($Pe<100$), or when the particle is near the bottom pole of the vesicle, the friction is most conveniently found from the noise in the particle trajectory. In the $t\to t_0$ (or $x\to x_0$) limit, the particle Brownian excursions are insensitive to gravity. This property is true everywhere on the vesicle surface.

Up until now, we have measured the friction

coefficients of latex spheres ($1\ \mu m \leq a \leq 8\ \mu m$) and glass spheres ($0.5\ \mu m \leq a \leq 2\ \mu m$) on SOPC ($L_\alpha$-stearoyl-oleoyl-phosphatidylcholine) vesicles ($15\ \mu m \leq R \leq 40\ \mu m$) at room temperature [5]. In the experimental protocol, we first measure the friction of the particle in bulk water (ζ_0) and then on the vesicle (ζ). Experimental data (see for instance Fig. 3) are consistent with our assumption that the friction is proportional to particle velocity; i.e., that ζ is constant. Of course, the ratio $\bar{\zeta} = \zeta/\zeta_0$ is found systematically >1, because of the membrane viscosity and the finite size of the vesicle. When $a/R \ll 1$, the finite size effect is negligible and the membrane shear viscosity (η) can be found approximately by using the theory worked out by Danov et al. [6] for a particle across a flat interface. By using this procedure, we found a set of dispersed values of η between 3 and 8×10^{-6} Poise [5]. This range is well in line with previous estimates based on fluorescence techniques (e.g., [9]).

Acknowledgments

We acknowledge financial support from the ULTIMATECH program (CNRS), the "Laboratoire Franco—Bulgare" (CNRS/Bulgarian Academy of Sciences/University of Sofia), the European Union, through Tempus JEP3949 and a fellowship to one of us (C.D.), and from the Bulgarian National Science Foundation through contract K-437/94. We thank P. Kralchevsky for useful discussions and M. Mitov for his help in development of the particle-tracking software.

References

[1] M.I. Angelova, B. Pouligny, G. Martinot-Lagarde, G. Gréhan, G. Gouesbet, Progr. Colloid Polym. Sci. 97 (1994) 293.
[2] C. Dietrich, M. Angelova, B. Pouligny, J. Phys. II France 7 (1997) 1651.
[3] M.I. Angelova, B. Pouligny, Pure Appl. Opt. A 2 (1993) 261.
[4] M.I. Angelova, D.S. Dimitrov, Prog. Colloid Polym. Sci. 76 (1988) 59; M.I. Angelova, S. Soléau, P. Méléard, J.F. Faucon, P. Bothorel, Springer Proc. Phys. 66 (1992) 178.
[5] K. Velikov, C. Dietrich, A. Hadjiisky, K. Danov, B. Pouligny, Europhys. Lett. 40 (1997) 405.
[6] K. Danov, R. Aust, F. Durst, U. Lange, J. Colloid Interface Sci. 175 (1995) 36.
[7] See for instance B.J. Berne and R. Pecora, Dynamic Light Scattering, John Wiley and Sons, New York, 1976.
[8] S. Chandrasekhar, Rev. Mod. Phys. 15 (1943) 1.
[9] J.F. Tocanne, L. Dupou-Cezanne, A. Lopez, Prog. Lipid Res. 33 (1994) 203 (and references therein)